

Nano-yttria in oxide dispersion strengthened tungsten under alpha particle irradiation

M.G. Petaccia^{*,a}, J.L. Gervasoni^{a,b}

^a Comisión Nacional de Energía Atómica (CNEA), Centro Atómico Bariloche (CAB), Av. Exequiel Bustillo 9500, San Carlos de Bariloche, Río Negro, Argentina

^b Consejo Nacional de Investigaciones Científicas y Técnicas (CONICET), Godoy Cruz 2290, Ciudad Autónoma de Buenos Aires, C1425FQB, Argentina

ARTICLE INFO

Keywords:

Primary radiation damage
Nuclear materials
ODS tungsten
Controlled Nuclear Fusion

ABSTRACT

Oxide dispersion strengthened (ODS) alloys, particularly steels and tungsten with yttria nanoparticles, have been proved to be a new class of high-strength nuclear material. We developed a simple model of an ODS tungsten alloy to study the primary damage produced by alpha particle irradiation on it. We show that the size of yttria nanoparticles embedded in a tungsten matrix is an important quantity to take into account under alpha particle irradiation. We explain the observed behaviors and we establish a critical scale parameter for the model we use, making a comparison with bulk tungsten.

1. Introduction

When considering a future fusion reactor, multiple interrelated problems must be evaluated. For the first wall of it, unique challenges in materials in extreme environments require advanced features in areas ranging from mechanical strength to thermal properties. The main challenges include wall life, erosion, fuel management and general safety. Tungsten (W) is the main material candidate for the first wall of a fusion reactor, since it is resistant to erosion, has the highest melting point of any metal and shows a fairly benign behavior under the irradiation of neutrons, as well as a low retention of tritium, among other properties.

One problem that can be quite crucial for complex components with multiple alloy materials and components is the recycling and activation under neutron irradiation. A potential problem with the use of W in a fusion reactor is the formation of radioactive and highly volatile WO₃ compounds, when irradiated by a neutron beam. To suppress the release of increased erosion of light elements and the mitigation of permeation and mechanical viability, a material (or alloy) compatible with neutron irradiation must be used. The Yttria permeation barriers is an element of low potential activation, so there is several recent work in this alloy, in Tungsten substrate [1].

Oxide dispersion strengthened (ODS) alloys, particularly steels and tungsten (W) with yttria (Y₂O₃) nanoparticles, have been proved to be a new class of high-strength nuclear material with high resistance to radiation [2–9].

ODS steels are a class of advanced structural materials with a

potential to be used at elevated temperatures due to the dispersion of thermally stable oxide nanoparticles into the matrix. ODS steels are resistant to radiation-induced swelling and have improved creep strength and oxidation/corrosion resistance at elevated temperatures compared to conventional steels [10].

On the other hand ODS Tungsten-based materials are candidate materials for structural applications in plasma facing components for future fusion power reactors [11,12]. It is also expected that such materials exhibit improved resistance to radiation damage, as the numerous interfaces between the particles and the matrix may act as sinks for the irradiation-induced defects [13].

However, the radiation resistance mechanisms associated with the embedded nanoparticles are still controversial and there are no consensus about these intrinsic mechanisms. For this reason, it is of interest to understand the process of localized radiation inside and around a Y₂O₃ nanoparticle. The interest in investigate these new materials in a fusion reactor is due to that the use of nuclear fusion reactions for electricity generation.

Future generation fusion reactors are based in the Deuterium–Tritium (DT) nuclear reaction. This process reaction products a 3.5 MeV α particle and a 14.1 MeV neutron. This amount of liberated energy makes that the materials, particularly the tungsten forming the first wall of the reactor, be exposed to extreme radiation conditions, given place to a severe radiation damage.

In this work we consider a model for an ODS tungsten-based material and we simulate the primary radiation damage produced on it by beam of alpha particles with energy of the order of 100 keV. In

* Corresponding author.

E-mail address: mauricio.petaccia@cab.cnea.gov.ar (M.G. Petaccia).

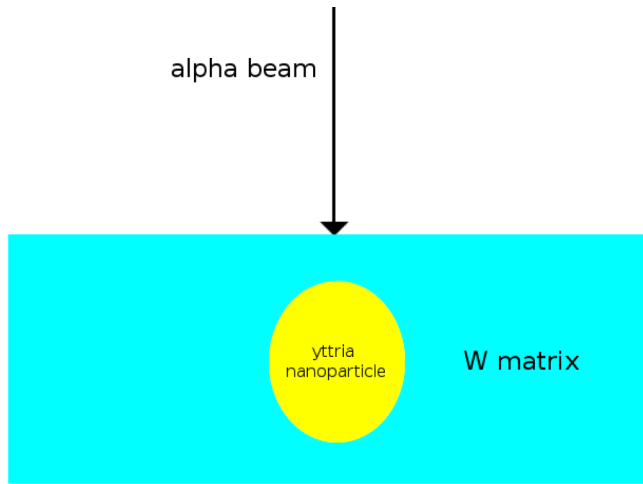


Fig. 1. Simulation scheme: An alpha particle beam focused on the target surface; the target is composed by an Y_2O_3 particle embedded in a Tungsten matrix.

addition, by making a comparison with results on bulk tungsten under the same radiation conditions we establish critical values for our model parameters.

2. Simulation methods

In order to analyze this situation, we assume a pure W matrix in which Y_2O_3 spherical nanoparticles are embedded, as is shown in Fig. 1. In this model of an ODS tungsten alloy, we apply the IM3D code to simulate the spatial distribution of radiation damage of the material due to alpha particle irradiation.

We use the so called Binary Collision Approximation (BCA) simulations [14], that are useful for examining the collisional stages of high energy cascades in statistically significant numbers. BCA simulations consider only the interactions between two colliding atoms at a time and in sequence. The computational program follows only the atoms having significant energies, using for this purpose a cutoff energy parameter, being thus very efficient. The BCA approach provides a good approximation to the collision stage, since it neglect many-body interactions that make small contributions to the atom trajectories at collision energies well above the atom displacement energy, which is typically about 25 eV for these materials [15].

Based on BCA, we choose the IM3D code [16]. It uses the TRIM-SRIM [17] database which has been extensively used to study different situations, such as wave guide fabrication [18], damage effects [19] among many others [20,21]. In addition, it offers the very useful alternative of parallel computing reducing considerably the CPU time. The code computes random trajectories of ions to give statistically meaningful data.

In this model, each trajectory corresponds to a single particle with a specified starting position, a given direction and an incident or primary energy. The particle is tracked as a random sequence of straight trajectories, ending in a binary nuclear collision event in which the particle changes its direction of motion and / or loses energy as a result of nuclear (elastic) and electronic interactions (inelastic). The energy and direction of the particle are updated by conserving energy and momentum. The probability of energy loss depends on the density of the target atom, as well as the nuclear and electronic forces that can be assumed to be independent of density. Meanwhile, point defects can occur in elastic collision events.

The projectile proliferation in a cascade does not continue indefinitely. At each collision, the projectile kinetic energy is subdivided into three contributions: (1) target atom kinetic energy; (2) reduced projectile atom kinetic energy; and (3) electronic excitation energy. As

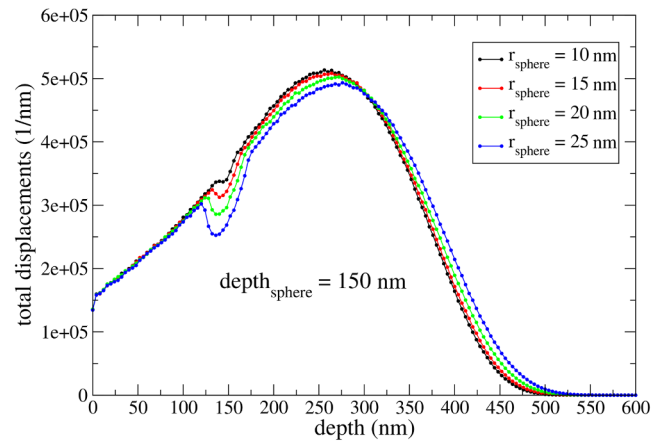


Fig. 2. Displacement depth distributions for different size spheres placed at 150 nm from the surface.

a consequence of this progressive energy subdivision, either one or both collision partners will eventually fail to induce a new collision and, as a consequence, the cascade eventually dies out.

We assume that the temperature of the bombarded material is $T = 0$ K, since the target atoms are in fixed positions at the beginning of each cascade; when the beam particles impinge the target, the temperature will locally rise but this heat will be conducted or radiated out to the surroundings, and the local temperature falls back to 0 K with no more atom movement

3. Results and discussion

We now focus on the results of simulations regarding the irradiation with 150 keV alpha particles of pure tungsten matrix bulk as well as ODS tungsten in which Y_2O_3 spherical nanoparticles are embedded. Of particular interest are distributions calculated from counting displaced atoms as a function of depth; these histograms are called displacement depth distribution functions and are discussed for selected cases.

Fig. 2 shows a comparison between the displacement depth distributions produced by alpha particles for an ODS tungsten alloy in which yttria nanoparticles have different radii. The region that is occupied by the nanoparticle is clearly seen, despite the total stopping power in Yttrium is larger than in Tungsten, as shown in Fig. 3; it is worth noticing that Yttrium is diluted with Oxygen in the Yttria compound, making the total displacements inside the nanoparticle diminished due to the abrupt change in the atomic density of the material,

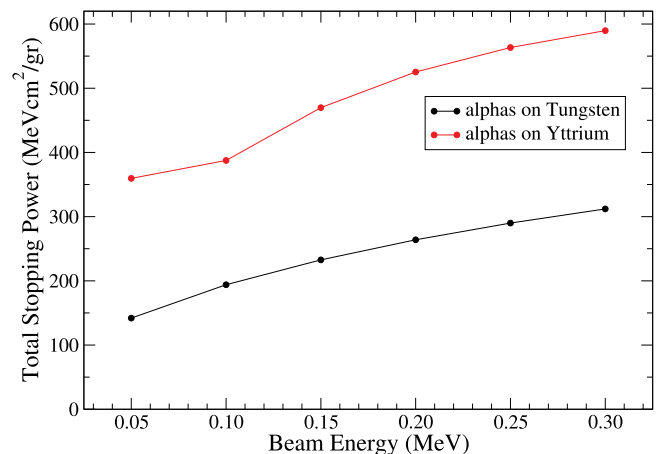


Fig. 3. Stopping power for alphas on Tungsten [22] and Yttrium [23] as a function of the beam energy.

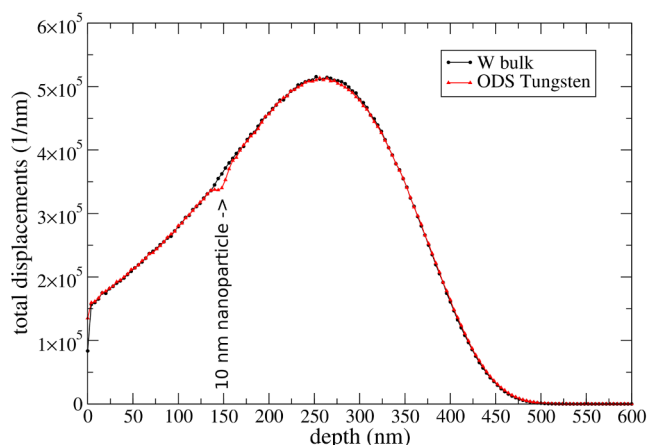


Fig. 4. Displacement depth distributions for bulk (black circles) and ODS (red triangles) tungsten. (For interpretation of the references to color in this figure legend, the reader is referred to the web version of this article.)

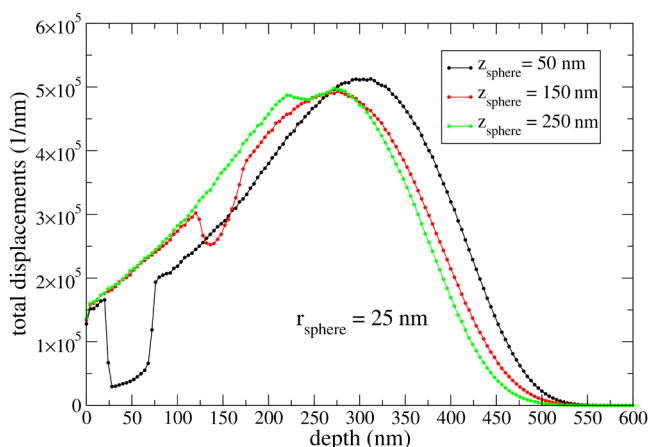


Fig. 5. Displacement depth distributions for ODS tungsten with particles of fixed radius (25 nm) placed at different depths.

this changes from 6.34×10^{22} atoms/cm³ in the tungsten matrix to 1.11×10^{22} atoms/cm³ inside the nanoparticle, an $\sim 82\%$ variation.

We observe that the maximum of the displacement depth distribution moves to larger depths as the radius of the nanoparticle increases. This effect is produced because, as the size of the nanoparticle becomes larger, the alpha particles of the beam enter the nanoparticle, traveling a larger region of lower density. In its trajectory, the alpha beam emerges back to tungsten with barely scattered trajectories.

In Fig. 4 we see a comparison of the displacement depth distributions for bulk tungsten and ODS alloy with 10 nm nanoparticles placed 150 nm beneath the target surface. It is worth emphasizing that in this particular situation the tail of each distribution shows the same behavior, i.e. displacements are produced within the same range in each material. This guarantee that adding small (~ 10 nm) particles at an adequate depth preserve the bulk response to primary radiation damage.

An interesting behavior is observed when a Y₂O₃ particle with a given radius is placed at different depths as shown in Fig. 5. When the nanoparticle is closer to the surface (50 nm), deeper primary damage is produced in the material: the alpha particle beam enter the target and travel a small distance before hitting the Y₂O₃ nanoparticle, the beam will not suffer a significant lateral spreading at this stage. After that the alpha particles move inside the yttria sphere they are not deviated from its original trajectory because Y₂O₃ atomic density is smaller than in bulk W; consequently the beam emerges at the opposite side of the

nanoparticle practically with the same energy and direction and continues the propagation in tungsten displacing atoms.

On the other hand, when the Y₂O₃ particle is far away from the target surface (250 nm), the displacement depth distribution tail is closer to the impact point: each alpha particle of the beam has a longer trajectory in W before reaching the yttria nanoparticle region, therefore the particle suffers more collisions and the beam as a whole spreads more in the lateral dimension than in the case previously discussed. As a consequence, the alpha particles enter the Y₂O₃ sphere from different angles. When they finally get out they move through the tungsten matrix producing atom displacements in several directions.

The situation where the 25 nm particle is placed at an intermediate distance of 150 nm it is also displayed in Fig. 5 and the distribution shows the expected behavior. Similar results are obtained in all the cases that we studied (as i.e., all the possible combinations of $r = 10$ nm, 15 nm, 20 nm and 25 nm with $z = 50$ nm, 150 nm and 250 nm).

4. Conclusions

In this work, we apply a simple and direct model of ODS tungsten alloy to study the effect of alpha particle irradiation on it. We show, under this simplification, that the size and depth of Y₂O₃ nanoparticles embedded in a tungsten matrix are important quantities to take into account under alpha particle beam irradiation.

We analyze the damage at different depth distributions produced by alpha particles. Considering all the cases under study we obtain a critical size (~ 10 nm) and position (~ 150 nm) for the nanoparticles for which the displacements distribution are similar to the ones for bulk tungsten.

Due to the importance of tungsten in future nuclear devices, there are some works describing its behavior [24–28]. In particular in [28] several experimental results are discussed regarding irradiation of structural and plasma facing materials, particularly bulk tungsten with alpha particles. We can qualitatively observe that the damage profiles are similar despite of the different irradiation conditions; in this work we use a much lower flux and beam energy than [28]. We choose a beam energy of 150 keV so that alpha particles can interact with W nuclei. In this sense work is still being done to improve the simulation method to be able to perform high flux and high energy irradiation on nanostructured materials.

The previous described chemical and physically complex processes (which should require more energy parameters ab initio than only one initial E) are beyond the scope of this work and could be analyzed in future studies, which are expected to give a more realistic characterization of the chemical mixture induced by radiation beyond the single-valued Binary Collision Approximation as a characterization of radiation damage.

Acknowledgments

This work was financially supported by Consejo Nacional de Investigaciones Científicas y Técnicas (CONICET) and by the Controlled Nuclear Fusion Program of the Comisión Nacional de Energía Atómica (CNEA) from Argentina.

Supplementary material

Supplementary material associated with this article can be found, in the online version, at [10.1016/j.nme.2019.100681](https://doi.org/10.1016/j.nme.2019.100681).

References

- [1] J. Coenen, S. Antusch, M. Aumann, W. Biel, J. Du, J. Engels, S. Heuer, A. Houben, T. Hoeschen, B. Jasper, et al., Materials for demo and reactor applications—boundary conditions and new concepts, *Phys. Scr.* 2016 (T167) (2015)

- 014002.
- [2] D. Blagoeva, J. Opschoor, J. Van der Laan, C. Sârbu, G. Pintsuk, M. Jong, T. Bakker, P. Ten Pierick, H. Nolles, Development of tungsten and tungsten alloys for DEMO divertor applications via MIM technology, *J. Nucl. Mater.* 442 (1–3) (2013) S198–S203.
 - [3] L. Fave, M.A. Pouchon, M. Döbeli, M. Schulte-Borchers, A. Kimura, Helium ion irradiation induced swelling and hardening in commercial and experimental ODS steels, *J. Nucl. Mater.* 445 (1–3) (2014) 235–240.
 - [4] D. Brimbal, S. Miro, V. de Castro, S. Poissonnet, P. Trocellier, Y. Serruys, L. Beck, Application of raman spectroscopy to the study of hydrogen in an ion irradiated oxide-dispersion strengthened Fe–12Cr steel, *J. Nucl. Mater.* 447 (1–3) (2014) 179–182.
 - [5] J. Chen, P. Jung, J. Henry, Y. De Carlan, T. Sauvage, F. Duval, M. Barthe, W. Hoffelner, Irradiation creep and microstructural changes of ods steels of different cr-contents during helium implantation under stress, *J. Nucl. Mater.* 437 (1–3) (2013) 432–437.
 - [6] Z. Huang, A. Harris, S.A. Maloy, P. Hosemann, Nanoindentation creep study on an ion beam irradiated oxide dispersion strengthened alloy, *J. Nucl. Mater.* 451 (1–3) (2014) 162–167.
 - [7] T. Lazauskas, S.D. Kenny, R. Smith, G. Nagra, M. Dholakia, M. Valsakumar, Simulating radiation damage in a bcc Fe system with embedded yttria nanoparticles, *J. Nucl. Mater.* 437 (1–3) (2013) 317–325.
 - [8] R. Liu, Z. Xie, Q. Fang, T. Zhang, X. Wang, T. Hao, C. Liu, Y. Dai, Nanostructured yttria dispersion-strengthened tungsten synthesized by sol–gel method, *J. Alloys Compd.* 657 (2016) 73–80.
 - [9] G. Odette, M. Alinger, B. Wirth, Recent developments in irradiation-resistant steels, *Annu. Rev. Mater. Res.* 38 (2008) 471–503.
 - [10] L.L. Hsiung, M.J. Fluss, S.J. Tumey, B.W. Choi, Y. Serruys, F. Willaime, A. Kimura, Formation mechanism and the role of nanoparticles in Fe–Cr ODS steels developed for radiation tolerance, *Phys. Rev. B* 82 (18) (2010) 184103.
 - [11] R. Neu, V. Bobkov, R. Dux, A. Kallenbach, T. Pütterich, H. Greuner, O. Gruber, A. Herrmann, C. Hopf, K. Krieger, et al., Final steps to an all tungsten divertor tokamak, *J. Nucl. Mater.* 363 (2007) 52–59.
 - [12] N. Baluc, Final report on the EFDA task tw1-ttma-002 deliverable 5, Assessment Report on Tungsten, (2002).
 - [13] M.-N. Avettand-Fenoel, R. Taillard, J. Dhers, J. Foct, Effect of ball milling parameters on the microstructure of W–Y powders and sintered samples, *Int. J. Refract. Met. Hard Mater* 21 (3–4) (2003) 205–213.
 - [14] W. Eckstein, Computer Simulation of Ion-Solid Interactions, 10 Springer Science & Business Media, 2013.
 - [15] G.S. Was, Fundamentals of Radiation Materials Science: Metals and Alloys, Springer, 2016.
 - [16] Y.G. Li, Y. Yang, M.P. Short, Z.J. Ding, Z. Zeng, J. Li, Im3d: a parallel monte carlo code for efficient simulations of primary radiation displacements and damage in 3d geometry, *Sci Rep* 5 (2015) 18130.
 - [17] J.F. Ziegler, M.D. Ziegler, J.P. Biersack, Srim—the stopping and range of ions in matter (2010), *Nucl. Instrum. Methods Phys. Res. Sect. B* 268 (11) (2010) 1818–1823.
 - [18] A. Bettiol, S.V. Rao, T. Sum, J. Van Kan, F. Watt, Fabrication of optical waveguides using proton beam writing, *J. Cryst. Growth* 288 (1) (2006) 209–212.
 - [19] G. Bentini, M. Bianconi, L. Correr, M. Chiarini, P. Mazzoldi, C. Sada, N. Argiolas, M. Bazzan, R. Guzzi, Damage effects produced in the near-surface region of x-cut linbo 3 by low dose, high energy implantation of nitrogen, oxygen, and fluorine ions, *J. Appl. Phys.* 96 (1) (2004) 242–247.
 - [20] M.T. Robinson, I.M. Torrens, Computer simulation of atomic-displacement cascades in solids in the binary-collision approximation, *Phys. Rev. B* 9 (12) (1974) 5008.
 - [21] R.E. Stoller, M.B. Toloczko, G.S. Was, A.G. Certain, S. Dwaraknath, F.A. Garner, On the use of SRIM for computing radiation damage exposure, *Nucl. Instrum. Methods Phys. Res. Sect. B* 310 (2013) 75–80.
 - [22] Report 90, J. Int. Commis. Radiat. Units Meas. 14 (1) (2016) NP–NP, <https://doi.org/10.1093/jicru/ndw043>.
 - [23] C. Williamson, J. Boujot, J. Picard, Tables of Range and Stopping Power of Chemical Elements for Charged Particles of Energy 0.5 to 500 MeV, Technical Report, Commissariat a l’Energie Atomique, 1966.
 - [24] S. Gonderman, J. Tripathi, T. Novakowski, T. Sizyuk, A. Hassanein, The effect of low energy helium ion irradiation on tungsten-tantalum (W-Ta) alloys under fusion relevant conditions, *J. Nucl. Mater.* 491 (2017) 199–205.
 - [25] S. Wurster, R. Pippan, Nanostructured metals under irradiation, *Scr. Mater.* 60 (12) (2009) 1083–1087.
 - [26] Y. Ueda, H. Lee, N. Ohno, S. Kajita, A. Kimura, R. Kasada, T. Nagasaka, Y. Hatano, A. Hasegawa, H. Kurishita, et al., Recent progress of tungsten R&D for fusion application in japan, *Phys. Scr.* 2011 (T145) (2011) 014029.
 - [27] M. Baldwin, R. Doerner, Formation of helium induced nanostructure fuzzon various tungsten grades, *J. Nucl. Mater.* 404 (3) (2010) 165–173.
 - [28] A. Ryazanov, V. Koidan, B. Khrpunov, S. Latushkin, V. Petrov, L. Danelyan, E. Semenov, V. Unezhev, Investigations of radiation damage effects on iter structural and plasma-facing materials, *Fusion Sci. Technol.* 61 (2) (2012) 107–117.